



# **LHCb Upgraded RICH 2 Engineering Design Review Report**

The LHCb RICH 2 Collaboration

**University of Cambridge, Cambridge, UK**

P. Garsed, S.A. Wotton

**University of Genoa and INFN, Genoa, Italy**

R. Cardinale, A. Petrolini

**University of Padova and INFN, Padova, Italy**

M. Benettoni, G. Simi, M. Zago

**Rutherford Appleton Laboratory, Chilton, UK**

S. Easo

**CERN, Geneva, Switzerland**

C. D'Ambrosio, C. Frei, J. He, D. Piedigrossi

## **Abstract**

During the Long Shutdown 2 of the LHC, the LHCb experiment and, specifically, its two Ring Imaging Cherenkov (RICH) detectors will undergo a major upgrade. RICH 2 will be refurbished with new photon detectors and their associated electronics, with the capability of up to 40 MHz sustained acquisition rate. A new support and cooling system has been developed for the two photodetector arrays, retaining the vessel, gas and optical systems unchanged. This document describes their new mechanical arrangement, its engineering design, installation and alignment. A summary of the project schedule and Institute responsibilities is provided.



# Contents

<b>1</b>	<b>Introduction</b>	<b>2</b>
<b>2</b>	<b>The MaPMT region</b>	<b>3</b>
2.1	Introduction and layout . . . . .	3
2.2	The T-piece of the photon detector column . . . . .	6
2.3	Support structure and assembly considerations . . . . .	9
2.4	MaPMTs services, routings and patch panels . . . . .	12
<b>3</b>	<b>Project planning</b>	<b>17</b>
	<b>Appendices</b>	<b>19</b>
<b>A</b>	<b>Appendix A: Cooling requirements</b>	<b>19</b>
<b>B</b>	<b>Appendix B: Radiation hardness</b>	<b>20</b>

# 1 Introduction

The LHCb experiment is undergoing a major upgrade [1], with data-taking expected to start in 2021. Two Ring Imaging Cherenkov (RICH) detectors, RICH1 and RICH2, provide particle identification over the 2-100 GeV/c momentum range Fig. 1. The RICH2 gas radiator, CF<sub>4</sub>, is contained in a vessel of  $\sim 100\text{ m}^3$  measuring 7 m wide  $\times$  2.3 m deep  $\times$  6.2 m high. In this vessel sits the optical system, which is composed of an array of 56 spherical mirrors of 8.6 m focal length, developing around the beam pipe. It focuses and guides out of the acceptance the Cherenkov photons towards two photodetector arrays, placed on the respective left- and right- focal planes by means of two arrays of 20 flat mirrors each. Two quartz plates separate the magnetically shielded photodetector boxes from the CF<sub>4</sub>-filled vessel. A drawing of RICH2 is show in Fig. 2.

In order to be compliant with the upgraded 40 MHz rates data acquisition, the present arrays made of Hybrid Photon Detectors (HPDs) have to be replaced. Multi-anode Photo Multiplier Tubes (MaPMTs) have been chosen as photodetector elements. A completely new readout electronics has been developed and designed to satisfy the challenging requirements of the LHCb experiment, still maintaining excellent single photon sensitivity and spatial resolution. The details of the project can be found in [1].

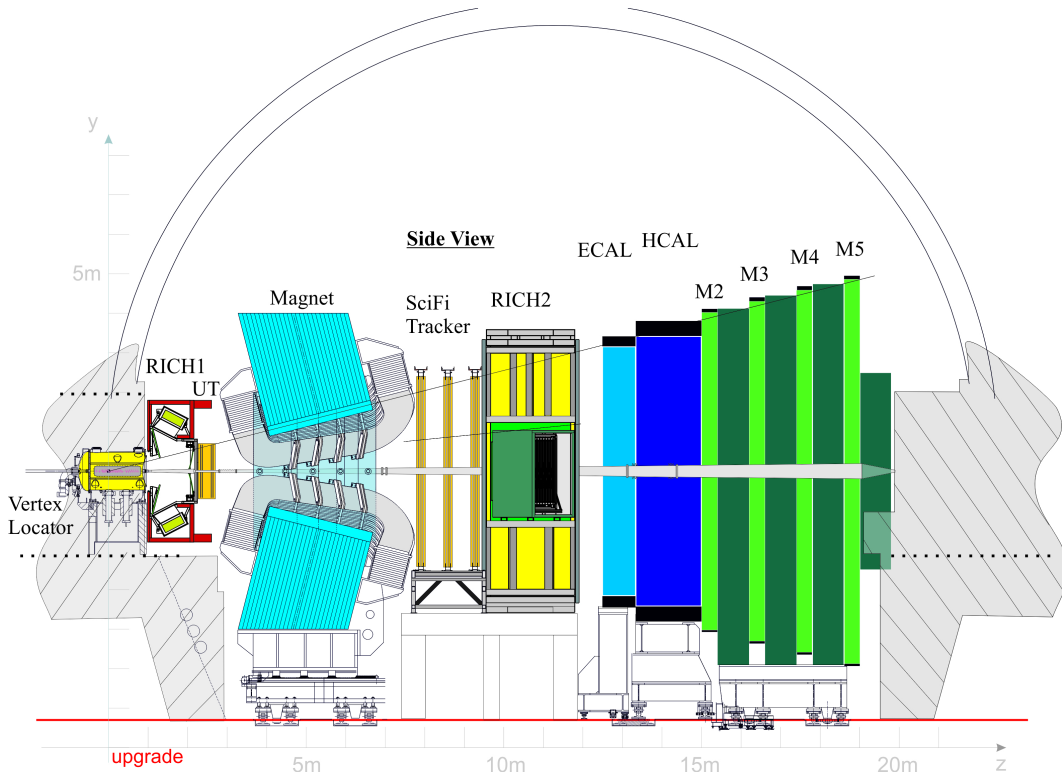


Figure 1: The LHCb upgraded detector [1], showing the location of RICH 2.

To efficiently utilize the 40 MHz readout rate, the instantaneous luminosity has to be increased to values up to  $2 \times 10^{33}\text{ cm}^{-2}\text{ s}^{-1}$ . Resulting occupancies vary from  $\sim 6\%$

in the central region of the arrays to less than 1% far from the beam pipe horizontal plane. In order to optimize resources and decrease complexity, simulations have shown that the particle identification performance of RICH 2 would be unaffected by using a coarser granularity in those low occupancy regions. Therefore, two different MaPMTs will be applied in RICH 2, namely models R11265 (1" size, 2.54 mm pixel size,  $8 \times 8$  channels) and R12699 (2", 6.25 mm pixel size,  $8 \times 8$  channels).

After a detailed introduction to the layout of the photodetector arrays (Section 2.1), this Engineering Design Report (EDR) will focus on the engineering design of all the elements which had to be changed with respect to the present configuration. Namely, these are :

- the column (Section 2.2), with its T-piece, which keeps together, supports and cools the MaPMTs and associated electronics;
- the array rack (Section 2.3), which supports the columns, provides stable and reliable metrics for the position identification of each photon, allows easy maintenance and extraction of columns during beam technical stops;
- the patch panels (Section 2.4) together with the necessary cables and services.

Throughout the previous sections a particular attention will be dedicated to the access, servicing and maintenance of the photodetector arrays and the consequent choices on mechanical solutions will be detailed. Finally, the overall project organization is detailed in Section 3 and two Appendices, A and B, are dedicated to the cooling and radiation considerations and testing.

This document is closely connected with the engineering design review of the upgraded RICH 1 detector [3]. As described in both documents, several choices have been taken jointly and, whenever allowed by the very different constraints, similar and/or identical schemes and components have been developed in order to optimize resources, simplify maintenance and reduce complexity [2].

## 2 The MaPMT region

### 2.1 Introduction and layout

As already mentioned in [3] much of the mechanics in the MaPMT region is shared between RICH 1 and RICH 2. However many of the space restrictions existing in RICH 1 are not present in the RICH 2 magnetic boxes, where ample space allows a more relaxed design. Moreover, the optical system is untouched and the MaPMT arrays can essentially be placed exactly at the same position as at present.

Two arrays of MaPMTs are present on the left (C-) side and the right (A-) side of the beam pipe as looking from the muon chambers to the VeLo detector Fig. 2. The two arrays are tilted on the horizontal plane at 1.065 rad w.r.t. the  $x$  axis (horizontal and perpendicular to the beam direction Fig. 3).

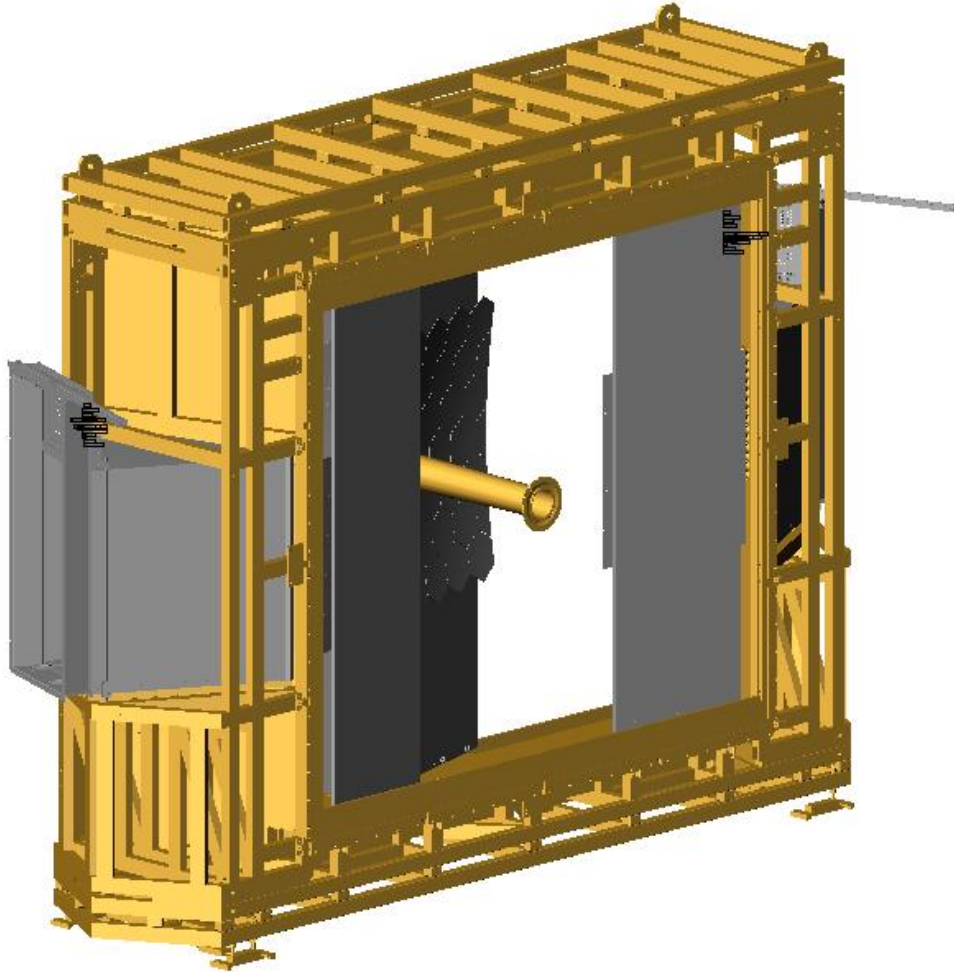


Figure 2: Left: CAD drawing of the existing RICH 2 detector.

The two arrays are composed by MaPMTs arranged in columns, as shown in Fig. 4. Each array is formed by 12 columns, placed side by side. For physics performance reasons, it is essential to minimize the pitch of this arrangement, at the same time assuring the integrity of the system when maintenance is required. The clearance foreseen between columns is 1 mm, which is deemed to be sufficient and safe. The column pitch is of 56 mm.

Each column can host 24 Elementary Cells (ECs). The EC is the basic mechanical and functional unit of the arrays. It provides mechanical support, magnetic shielding and thermal transfer for the MaPMTs and it contains the front-end electronic readout. In RICH 2 two types of ECs are present, called  $EC_R$  and  $EC_H$ , depending on the type and number of MaPMTs which they will host. Details of them can be found in [4]. Here it suffices to say that  $EC_R$  hosts 4 MaPMTs ( $4 \times 1''$ , Model Hamamatsu R11265, 256 channels Fig. 5 (left)), while  $EC_H$  only one ( $2''$ , Model Hamamatsu R12699, 64 channels Fig. 5 (right)). The ECs of both types retain exactly the same envelope and internal structure,

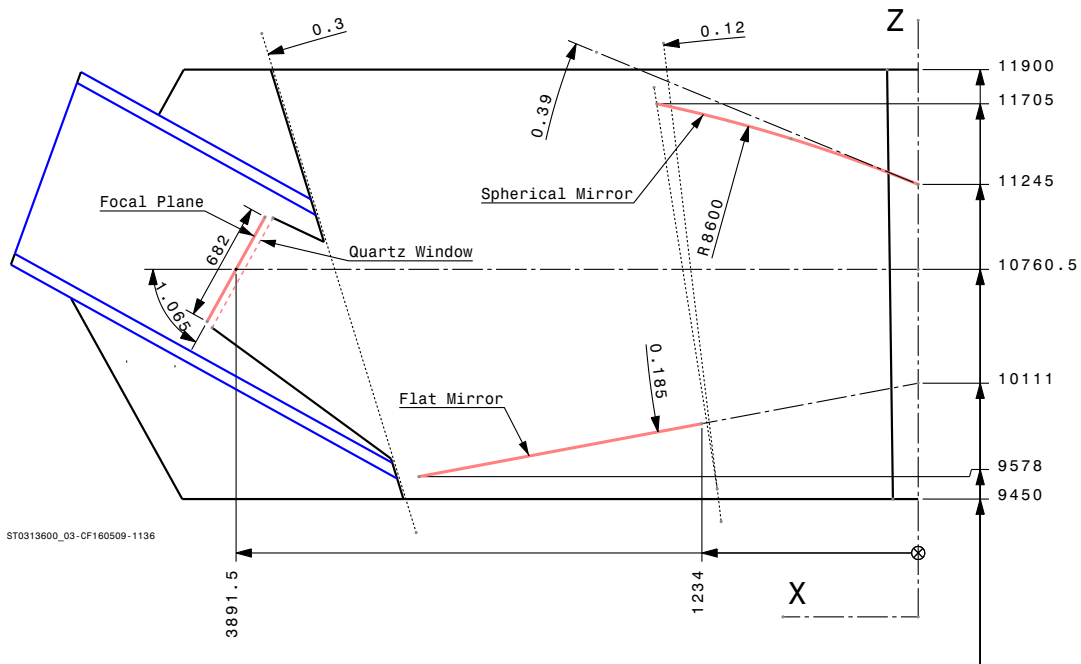


Figure 3: Half view of the RICH 2 optical layout in the  $x - z$  projection.

allowing for mechanical simplification, maintenance ease and resources optimization [5]. 1" MaPMTs are located in the middle third of the column, thus 8  $EC_R$  at the center of the column, while the 2" MaPMT are located at the two top and down third, thus 16  $EC_H$  per column.

Again it is to be noted, that the array sizes between RICH 1 and RICH 2 are almost identical, even though their acceptance coverage is much different (300 mrad in RICH 1 and 120 mrad in RICH 2). As discussed in [5], the particle identification performance of the LHCb RICH system is not worsened by the use of larger MaPMTs in the peripheral regions of the RICH2 arrays.

The binary signals detected by the ECs are sent to Digital Boards (DEBs), which have the task of acquiring, serializing, packing and send them to the computing facilities via dedicated optical links. The DEBs configure and control the front-end electronics. In RICH 2, as for the ECs, two types of DEB are present,  $DEB_R$  and  $DEB_H$ , according to the MaPMT types they readout. Two DEBs, type R, placed one in front of the other, are tasked to readout 16 x 1" types, while only one  $DEB_H$  reads 4 x 2" MaPMTs. The mechanical envelope of the DEB types is exactly the same (as for the ECs). However, owing to the much smaller number of bits per second to be readout, the  $DEB_H$  contains a reduced number of electronic components. The functional element after the EC is called Photon Detector Module (PDM), containing in its R-type configuration 16 x 1 MaPMTs, 512 CLARO chips and two  $DEB_R$ .

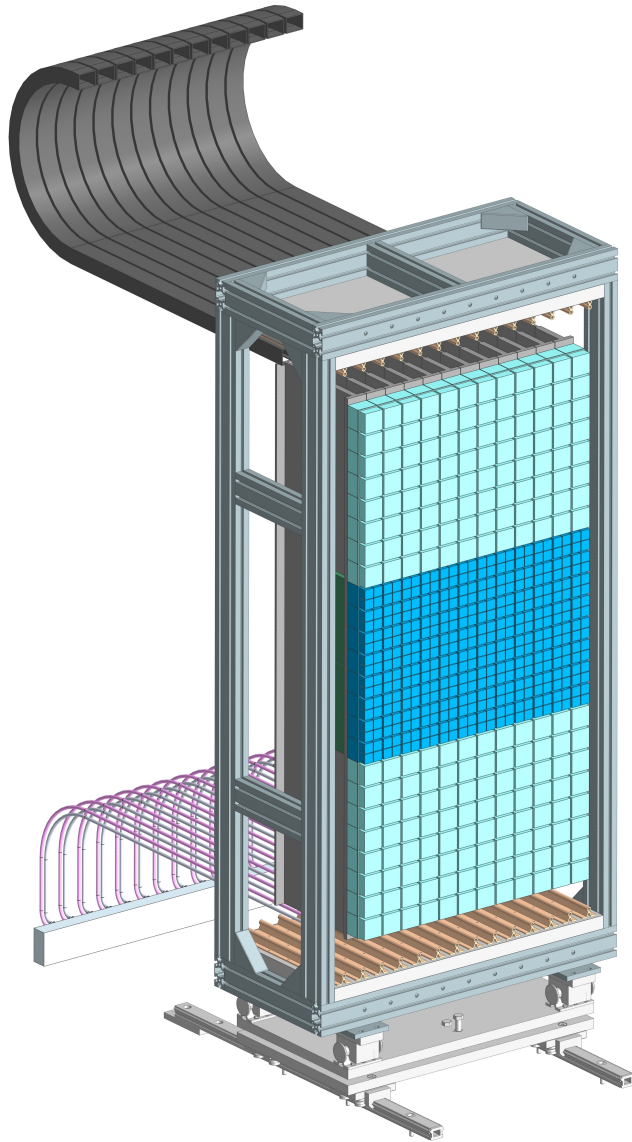


Figure 4: A CAD representation of the photodetector array.

## 2.2 The T-piece of the photon detector column

The structural backbone of the columns is an aluminum T-piece that realizes also the thermal exchange and transfer of heat between the various active components of the column. This is achieved by means of a coolant circulation inside two ducts, which run along the axis of the T-piece (also called cold-bar, to highlight its two functionalities). A drawing of the T-piece is shown in Fig. 6 (Right) *in light gray*, together with a blade (harness support) *in dark gray*, which increases stiffness of the vertical column and accommodates the numerous cables.

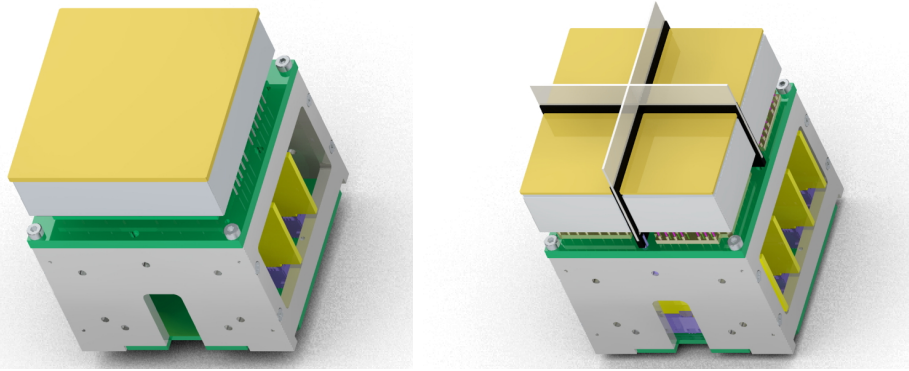


Figure 5: (Left) An Elementary Cell type  $EC_H$ ; the scale is indicated by the four mounted 1-inch MaPMTs (in orange). (Right) An Elementary Cell type  $EC_R$ .

Table 1: MaPMT and electronics quantities.

<b>The detailed functional element catalogue of one RICH 2 arrays</b>	
Columns:	12
Elementary Cells (ECs) per column:	24
Elementary Cells, H-type ( $EC_H$ ):	16
Elementary Cells, R-type ( $EC_R$ ):	8
$DEB_H$ :	4
$DEB_R$ :	4
$PDM_H$ :	4
$PDM_R$ :	2
ECs per column:	24
MaPMTs, H-type (2" inch) per column:	16
MaPMTs, R-type (1" inch) per column:	32
ECs per array:	288
<b>For the whole of RICH 2, baseline of 12 columns per array</b>	
Total number of Elementary Cells:	576
Total number of $EC_H$ :	384
Total number of $EC_R$ :	192
Total Number of MaPMTs, H-type:	384
Total Number of MaPMTs, R-type:	768

The T-piece present in RICH 2 is identical to the one shown in the RICH 1 EDR [3] and detailed in Section 5.3 of the same report. The differences are seen only at the level of the service support (blade), as the columns are hanging vertically for RICH 2 and horizontally for RICH 1, requiring therefore a different scheme. In what follows, many arguments will overlap with the discussion in [3]. Therefore, we shall try to complement and enrich the various aspects which characterize the design, wherever possible.

The T-piece is a precision mechanical piece, which provides direct reference for the

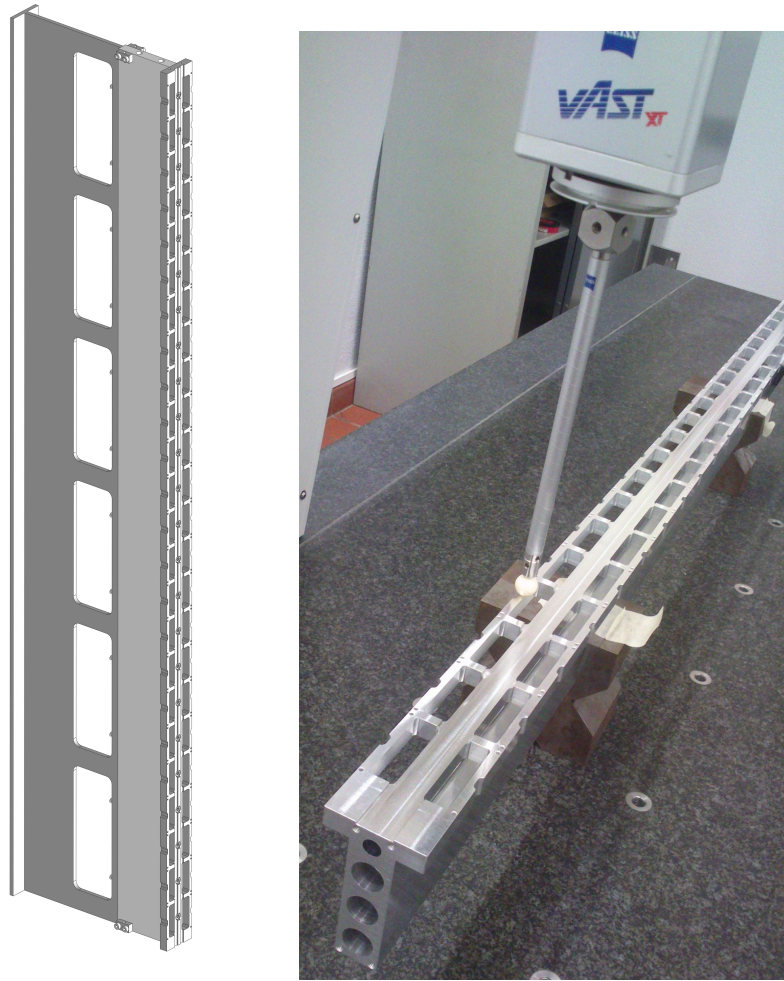


Figure 6: (Left) A CAD view of the T-piece. (Right) View of the T-piece full scale prototype on a stationary coordinate measuring machine.

ECs and the DEBs, both being placed on the opposite sides of the T-piece base (Fig. 6). The height of a column is 1400 mm, its depth and thickness  $10\text{ mm}$  and 55 mm respectively. A full-scale prototype of the T-piece was produced and tested and satisfied the strict specifications, imposed by the mechanical design (this is shown in Fig. 6, Left, note the number of four holes in this first design and the fact that it is built in only one piece). This prototype has been shown to comply better than 0.2 mm with flatness and parallelism of EC and DEB faces. The pitch of the slots for EC connectors better are than 0.1 mm [7].

The cooling ducts are two 10 mm diameter holes, one for go and one for return. They are deep-drilled into the spine of the cold-bar. A total drill depth of 1400 mm is achievable by drilling from either end. Prototype pieces have been successfully produced and the tolerances associated with deep drilling are acceptable ( $<0.5\text{ mm}$  off axis drift seen at the meeting point). The cooling is provided from the bottom end of each column and runs back and forth on the two ducts, thus the temperature distribution achieved along the bar

is more uniform than for a single duct and the expected MaPMTs temperature is about 30 °C. At the top end of the column, a return bypass is machined in the end-block that serves to connect the two ducts and provides the interface to the support trolley. Tightness is ensured by industrial grade O-rings sealing between the head of the cold-bar and the interface block. Tests are ongoing to further improve thermal exchange between coolant and ducts, investigating influence of coolant type, duct diameter, duct cross section shape and effect of baffles inside the ducts, with constraint to keep the pressure drop below 0.7 bar (see Appendix A).

### 2.3 Support structure and assembly considerations

The array structural support is a custom designed rack (Fig. 4). The rack for both left and right arrays are close to identical; all functionality and performance is maintained when inverted and only nominal variations are envisaged. The two racks are frames composed by structural commercial aluminum extruded profiles, bolted together by brackets and corner pieces that provide the needed stiffness and assembly precision.

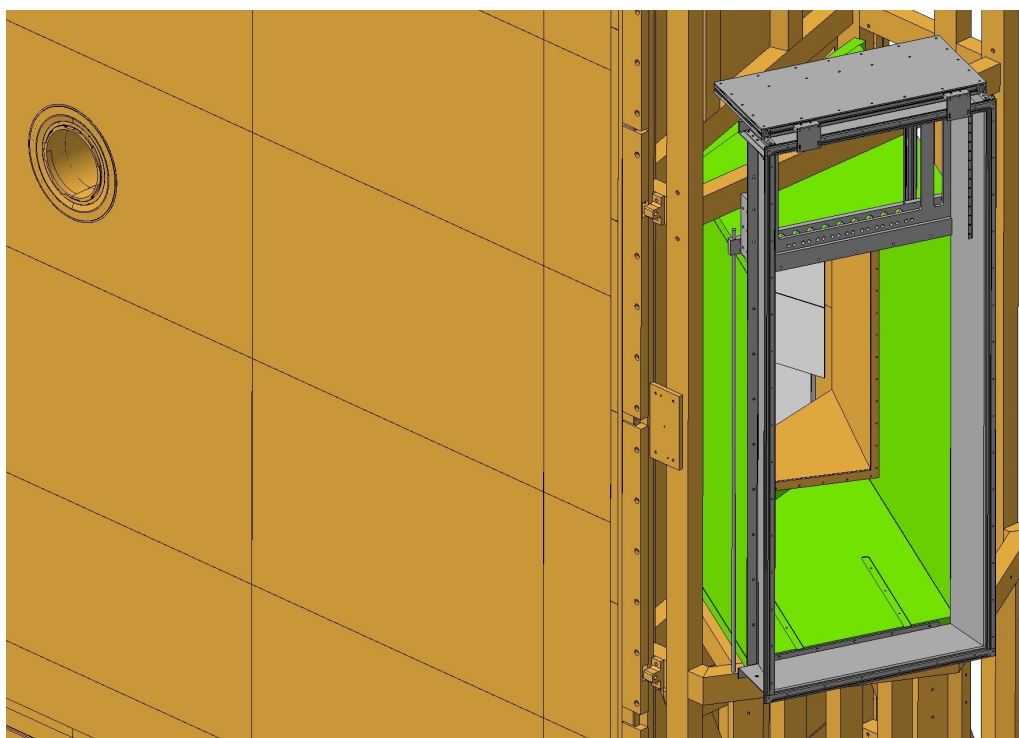


Figure 7: View of the magnetic shield and the extension frame.

The baseline rack layout is similar to the rack that host the current detector array [6]. As the existing ones, they are movable on rails with a movement in the direction perpendicular to the quartz window, in order to extract the racks from the photon detector enclosure, thus improving access for maintenance. A fine adjustment mechanism at the basement

to tune the alignment of the array versus the nominal position is also envisaged. Fig. 7 shows the existing magnetic shield box where the detector array will be installed (See also Fig. 2).

Each column in the rack runs on two dedicated rails, thus each column can be extracted individually by retracting it by hand. At each end of the column the cold bar is fixed to a trolley composed by an interface plate and two open cylindrical bearing that slide on cylindrical rails. The rails on which the MaPMT columns are sliding (slide systems) are precisely fixed to machined plates mounted on the rack bottom and top. This ensure proper precision to the position and relative pitch of the column versus rack structure and versus each other. Bearings are foreseen to be commercial bearings made of low friction polymer, offering the advantage to electrically isolate the ground of the cold bar thus allowing to choose the correct grounding scheme and preventing ground loops.

Rails are also commercial extruded rail profiles, made of hard anodized aluminum that reduce friction to acceptable values and further reduce risk of accidental electrical contacts between rack and columns. A CAD model of a rack is shown in Fig. 8 (Left). Fig. 8 (Right) shows a prototype of the rack prepared for laboratory tests.

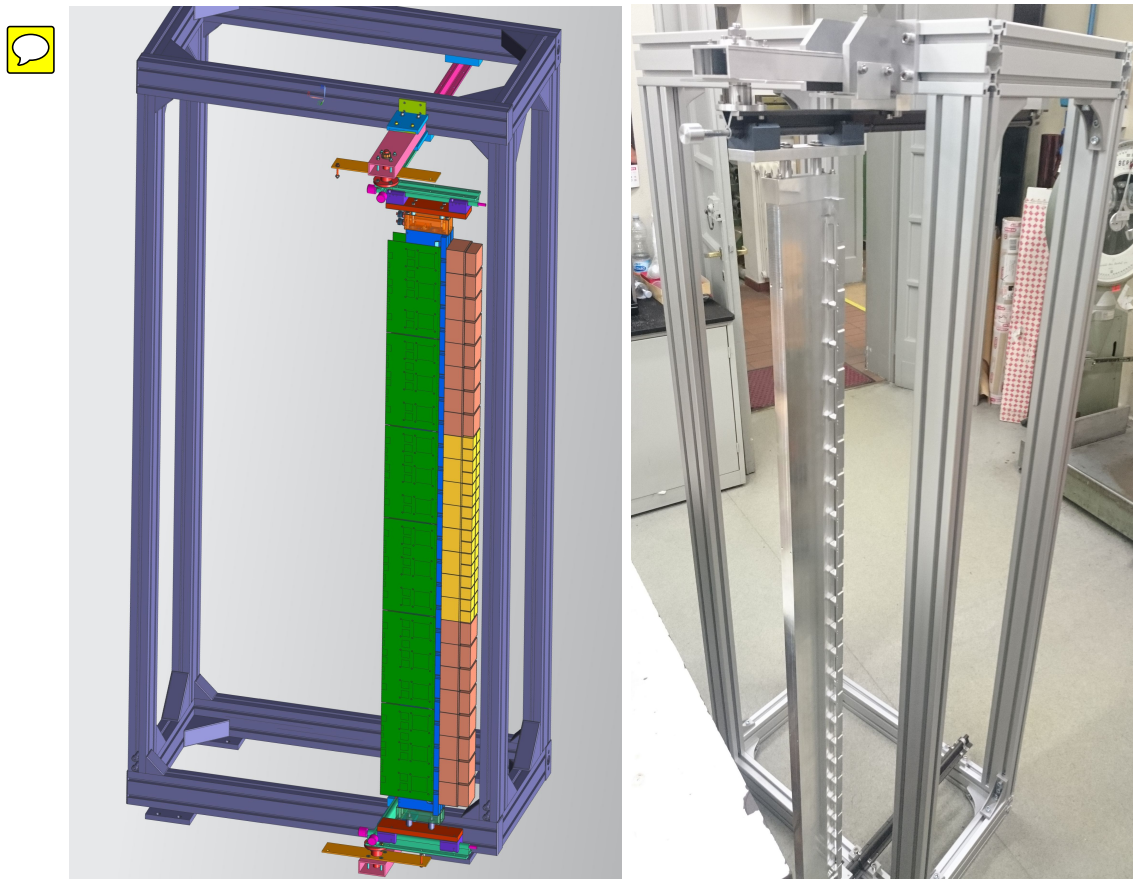


Figure 8: (Left) A CAD model of the rack for the MaPMT columns. (Right) View of the prototype rack for testing the column sliding system.

The ECs are screwed on the front face of the T-piece base. They are in thermal contact with it and their connectors spouse the equivalent connectors of the DEBs, placed internally to the T-piece. The digital boards (DEBs) are mounted on both sides of the Cold-bar and are thermally and mechanically coupled to it by means of interface plates (called Levelling Plates, see Fig. 9). These are machined and shaped in order to ensure a full thermal contact between dissipating components on the DEBs and the cold surface of the T-piece. For the part of the column occupied by H-type ECs, DEBs will be present only on one side of the T-piece (Fig. 14).

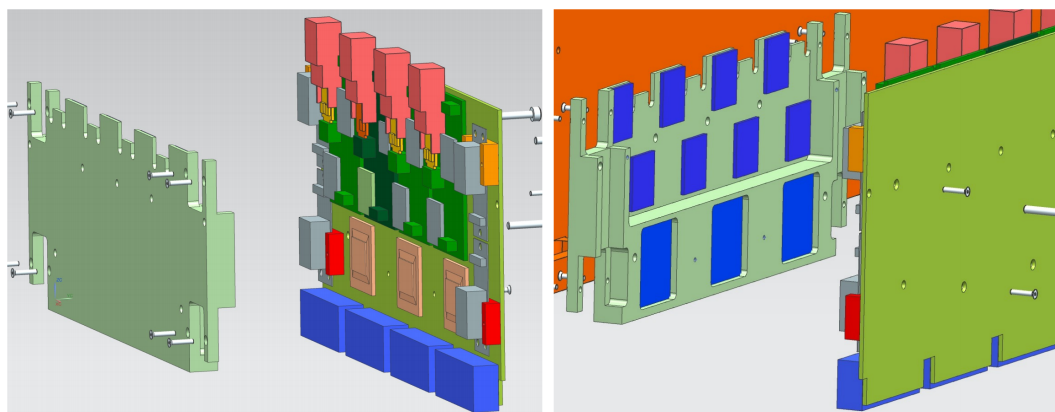


Figure 9: A CAD model of the digital electronic board with the leveling plate.

Cold-bars are positioned vertically and constrained by bearing at both ends. Loads on them is given by their own weight, weight of ECs, DEBs, cables, cable chain and services. The ECs, each of which weights  $\sim 0.25$  kg, are fixed directly to the Cold-bar by means of four M2 screws. The expected column mass is of the order of 20 kg.

Columns can be moved on the rails and manipulated by hand until it is required to fully remove them from the rack. Each individual column will be fully assembled in workshop/laboratory conditions to minimize risks and maximize quality assurance. The rack itself will be prepared in a laboratory and moved to the detectors once ready and tested. End stops will be included at the ends of the rails. They will be used to fix and locate via via set-screws individual column positions along the rail axis. The end stops will only need to be set at the time of initial installation and will be repeatable thereafter (Fig. 10).

The pitch between bearing pairs mounted at the two ends of each column and the pitch between the rails dedicated to each column can be affected by small deviation due to mechanical tolerances and/or differential dilatation due to non-uniform temperature. In order to compensate such tolerances, the bearing at one column end will be fixed to the cold bar allowing a small axial degree of freedom. Such clearance is recovered by preloaded washers springs acting between the floating trolley and the cold bar end, in order to realize a more precise coupling between cold-bar and trolleys and therefore a more precise positioning. The column movement can be affected by stick-slip effects due to the large distance between rails and relatively small distance between bearings on the same



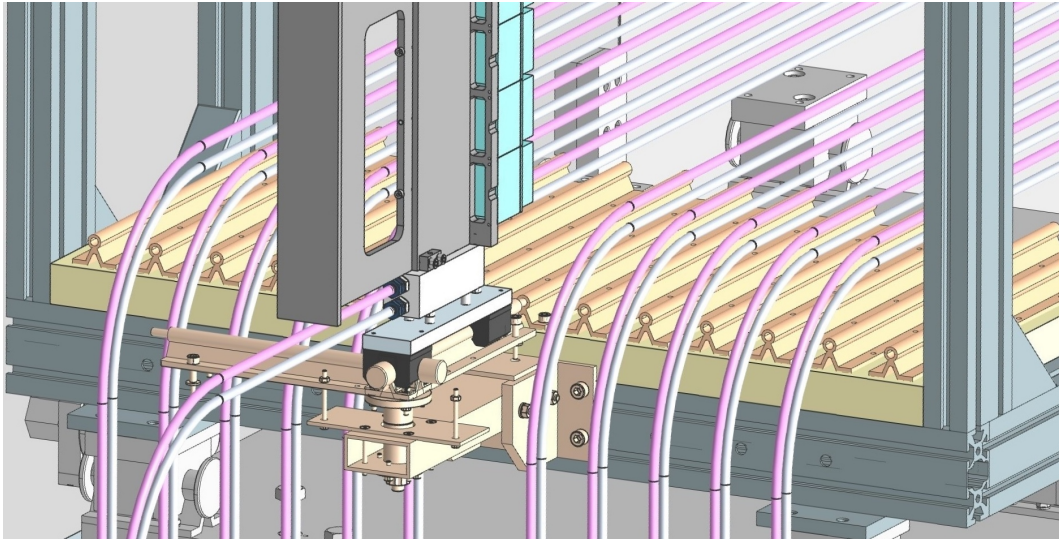


Figure 10: Close-up on the column sliding and cooling systems.

rail. The current baseline foreseen that the bars are suspended to the top rails and put under traction by the preload on the bottom bearings, in order to compensate backlash between bearings and rails thus improving movement smoothness 

Two extension rails can be provisionally mounted and aligned to the rails of the column to be extracted, allowing to increase extraction stroke and improving access to DEBs and ECs. The extension rails are mounted on two arms that are fixed to the top and bottom profile of the rack. When extracted on the extension rails the column is accessible all around in order to allow replacement of DEBs and ECs. The extension rails are coupled the support arms by a vertical support axis, that allow the column, when extracted on the extension rails, to be partially rotated around a vertical axis on both directions, further improving the access to both ECs and DEBs (see Fig. 11)  

## 2.4 MaPMTs services, routings and patch panels

As already described in [6], the instrumented columns have to be serviced by High and Low Voltages (HV and LVs), data and control fibres, monitoring cables and cooling support. All these services will use the service support (blade) and a commercial cable chain per column to be routed towards a single patch panel per array, situated above the magnetic shielding box. Fig. 11 shows the photon detector enclosure formed by the magnetic shield and an extension supporting the patch panel. The patch panel will be gas and light tight, as the current one, using proper feedthrough, connectors and fittings, eventually sealed. The requirement for some gas tightness stems from the need of controlling the atmosphere in the box, which are permanently flushed with  $N_2$  and kept at the lowest possible degree of humidity.

Services run of both sides of the cold-bar, it is thus possible to separate delicate services from bulky and stiff services. Thus, the LV cables and the fibers are placed on opposite

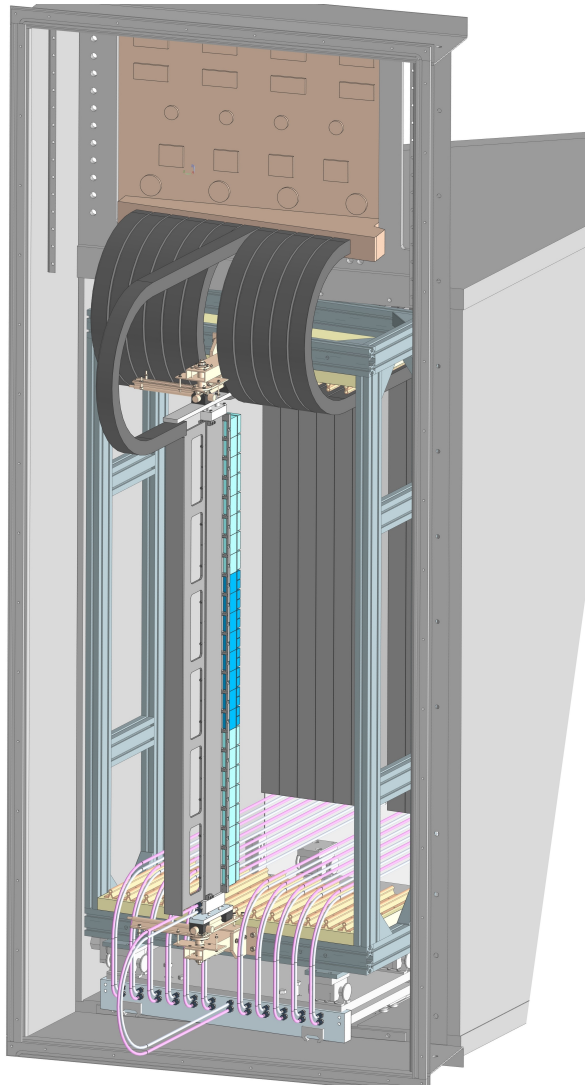


Figure 11: Integration view of the new photon detector system inside the enclosure.

faces, while the HV pigtails, local patch panels and cables are placed according to the space available that is mostly on the LV side. For all these routes, extensive CAD modelling has been undertaken, including bend radii, fiber diameter, connector access, constraints on equalized pigtails length, single fibers length, etc.

In detail, the various routing types (see Fig. 12):

1. LV power supply: one power line per board(s) of each PDM (board(s) serving 4 cells, 6 lines/column, *black and red cables*).
2. HV supply and lines: 1 line per PDM (4 ECs), 6 lines/column (*gray and blue cables*); per each PDM one small patch panel is foreseen nearby. Pigtails (*yellow and white wires*) of ECs are required to have the same length (per each of the two ECs types)



in order to have all identical ECs, thus arrangement of HV pigtails is affected by extra-length due to this constraint.

3. Data fibers: 1×12-fold splicer for data fibers/PDM. Two DEBs produce 6 data fibres each. Fibers between DEBs and splicers should be identical in length for procurement and spare variety reasons, this affects the routing of the fibers on the cold bar as a result of the extra-length to accommodate (*light blue fibres*).
4. Trigger and control fibers. For each two DEBs is foreseen one small splicer where TR/CO fibers of 2 DEBs are collected. Fibers between DEBs and splicers should be identical in length for procurement and spare variety reasons (*purple fibres*). 

For the fiber services, all fibers will be routed from the individual digital boards along a column towards the splicer, that collect single fibers from two boards. Bundled fibers connect the splicer to the patch panels Fig. 13. Looking end-on, all pipework and connectors must stay within the envelope of the column that they serve. This allows an individual column to be disconnected and accessed without disturbing its neighbours. Finally, a full cable column is shown in Fig. 14

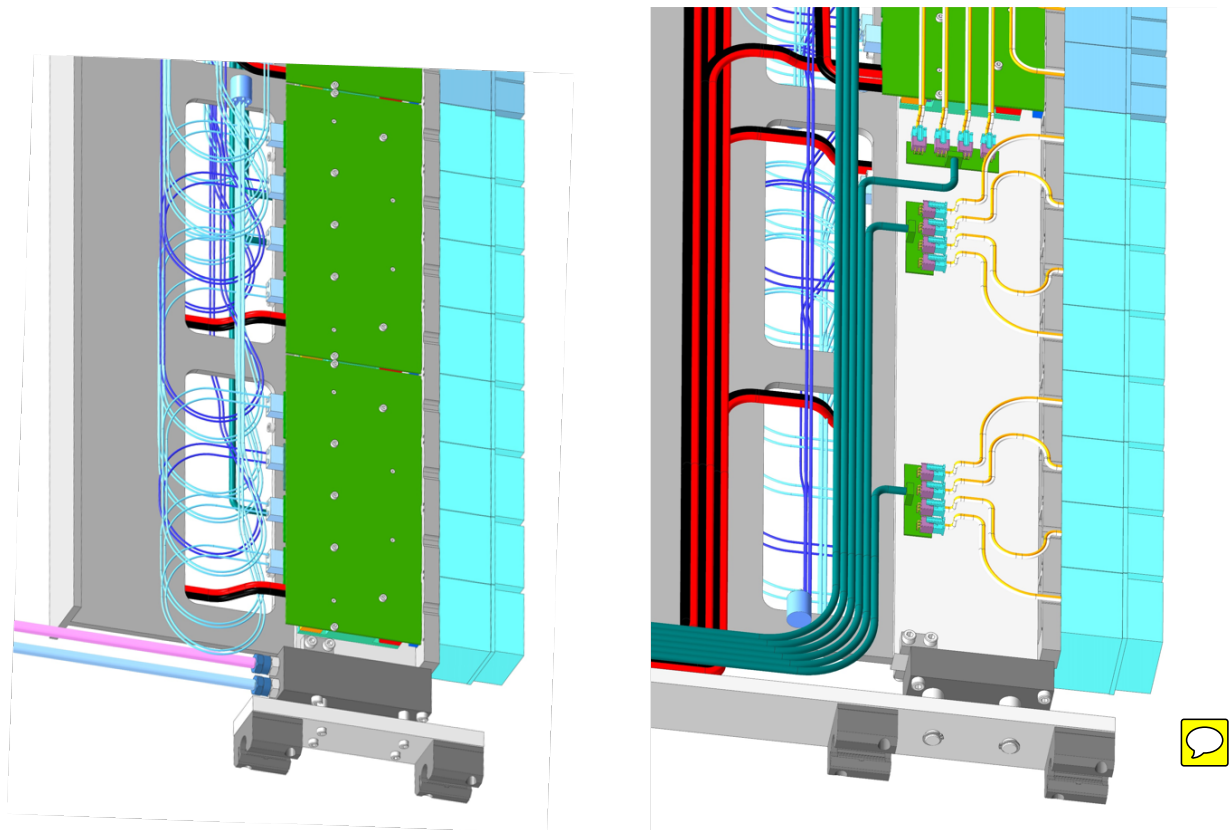


Figure 12: (Left) CAD view of possible routing of the fibers, LV and HV on the column.

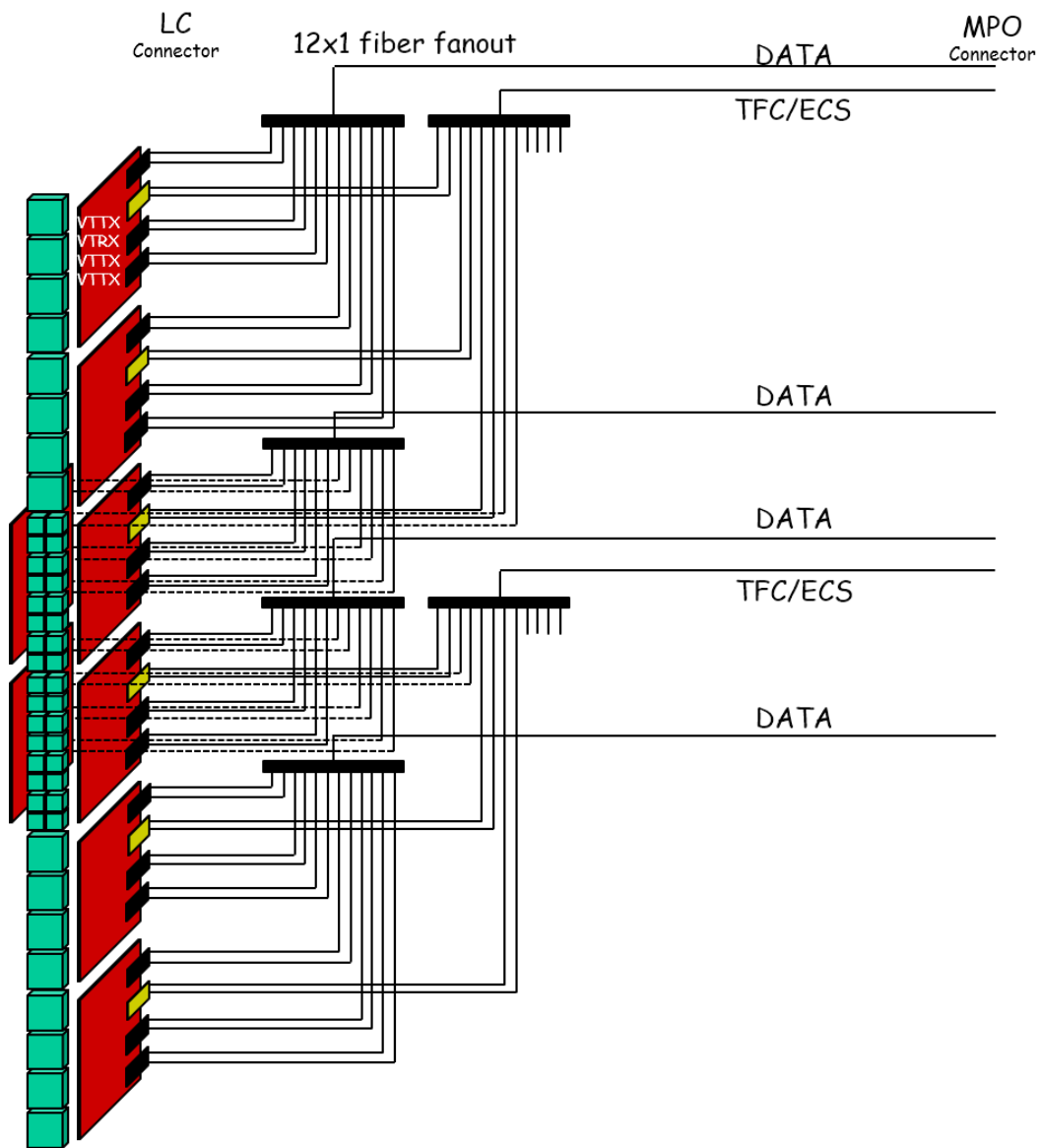


Figure 13: Schematic of the fiber connections

Cooling will be routed from the bottom with flexible hoses having extra length that allow the extraction of the rack or/and of the single columns for maintenance. Each array will be provided of a manifold placed inside the magnetic box for easy access and maintenance (see Fig. 10, 11).

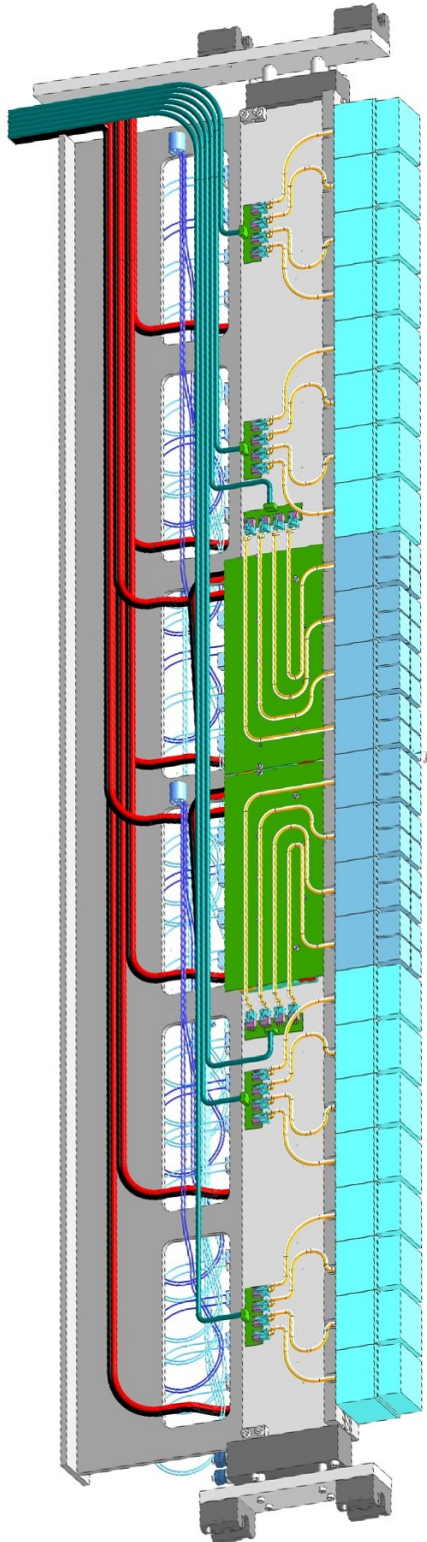


Figure 14: View of the column including the routing of the optical fibers.

### 3 Project planning

The following lists indicate the institutes responsible for delivery of the various work packages and their required completion dates. The parts of RICH2, which do not need modifications, remain under the present responsibility plan.

Table 2: Work packages and required completion dates.

---

**MaPMT assemblies**  
including mounting frame, columns and cooling assemblies.  
**Lead institute:** CERN  
Critical dates:

	<b>PRR:</b>		Apr 2017
	<b>MaPMT support ready to receive modules:</b>		May 2018
	<b>Installation:</b>		Mar 2020
1.1	MaPMT mounting frame final design	CERN, Padova	Nov 2016
1.2	MaPMT mounting assembly and rail structure	Padova	Nov 2016
1.3	Cooling system design	CERN, Padova	Nov 2016
1.4	Patch panels	CERN	Nov 2016
1.5	Production drawings and PRR	CERN, Padova	Apr 2017
1.6	Tender	CERN, Padova	July 2017
1.7	Production	CERN, Padova	May 2018
1.8	Install cooling system	CERN, Padova	Jan 2020
1.9	Assembly and alignment	CERN, Cambridge, Genova, Padova	Jan 2020
1.10	Installation	CERN, Genova, Padova	Mar 2020
1.11	Monitoring, alignment, radiation, environment		
1.12	Metrology	CERN	Feb 2020
1.13	Detector safety interlocks	CERN	Feb 2020
1.14	Radiation test coordination	CERN	Ongoing

---

**Handling tools**  
including mounting frame, columns and cooling assemblies.  
**Lead institute:** CERN, Padova  
Critical dates:

	<b>As required to execute assembly tests:</b>		Mar 2019
	<b>As required to facilitate installation at IP8:</b>		Aug 2019
2.1	Including mounting frame, columns and cooling assemblies.	Padova	Jan 2019
2.2	Installation procedures for MaPMT columns	CERN, Padova	Jan 2019

## Acknowledgments

We are indebted to our collaborators of the RICH 1 EDR for the stimulating discussions, close collaboration and warm working atmosphere, which have characterized the development and realization of both Upgraded RICH EDRs. We would also like to thank M. Fiorini of the University of Ferrara for his work on the RICH 2 radiation studies.

# Appendices

## A Appendix A: Cooling requirements

The cooling system of RICH 2 is the same as for RICH 1 [3]. All considerations and plans reported there can be equally applied to RICH 2, except for the absolute values of dissipated power per column and in total. This is due to the particular column structure of RICH 2, where two different MaPMT models are employed. Therefore, we shall not repeat what already stated in the RICH 1 EDR and Cooling System Report [8], rather only specific heat sources values and ensuing requirements for RICH 2 are addressed here.

The heat power generated by all active components of RICH 2 photon detector assembly (PDA) is accounted in Table 3. Table 4 summarizes the main requirements of its PDA cooling system.

Table 3: RICH 2 heat power of the front-end electronics.

Component	Power
Digital Boards, LV (7 V, 3.4 A):	3.6 kW
Front-end ASIC Boards (0.128 W/board)	150 W
The high voltage divider boards	650 W
Total power per Column	175 W
Total power	4.2 kW

Table 4: Requirements of the RICH 2 cooling system.

Number of circuits (loops):	2
Nominal heat power:	$2 \times 2.1$ kW
Max. temperature of the photon detectors:	$< 35$ °C
Max. temperature of electronics	$< 50$ °C
Coolant (Fluorinated fluid) [9]:	3M Novec™ 649, 7100 or C <sub>6</sub> F <sub>14</sub>
Heat transfer medium:	Liquid mono-phase
Minimum temperature at the PDA inlet:	$\sim 11$ °C
Temperature difference of the coolant (PDA), $\Delta T_{inlet-outlet}$ :	5 °C
Maximum pressure at the PDA inlet:	$< 2$ bar
Pressure drop in the PDA:	$\sim 0.7$ bar
Leak rate, in total:	$< 0.05$ l/day
Typical flow of the coolant:	1060 l/h

## B Appendix B: Radiation hardness

We will again limit ourselves to the RICH 2 specificities, kindly asking the reader to refer to the aforementioned EDR for RICH 1 [3] for the general consideration on the Upgraded LHCb radiation environment. All numbers are calculated considering a 10 year accumulated  $50 \text{ fb}^{-1}$  integrated luminosity. Geometry and materials used in the simulations for RICH 2 are as for the current system [10]. However, an LHCb model, without the Pre-Shower (PS), Scintillation Pad Detector (SPD) and Muon1 detectors has been investigated to highlight the expected increase of the neutron equivalent dose [11]. As a general assumption, for a specific region corresponding to a well-defined RICH component, the worst case value of the corresponding radiation distribution is considered. Finally, only the results on RICH 1 (See Appendix B of [3]) are reported when these can be taken as upper limits for RICH 2 (in any case they are of the same order of magnitude).

From the simulations, in the photon detector region of RICH 2, we should expect a total ionizing dose of 0.8 kGy, a neutron fluence of  $3 \times 10^{12}$  1 MeV  $n_{eq}/\text{cm}^2$  and a HEH fluence of  $0.5 \times 10^{12} \text{ cm}^{-2}$  [12]. At the central region of the RICH 2 (30 cm from the beam line), the expected average TID is about 10 kGy, the 1 MeV neutron equivalence fluence is about  $400 \times 10^{11} \text{ cm}^{-2}$ , while the HEH fluence is about  $150 \times 10^{11} \text{ cm}^{-2}$  [11].

The components which will be exposed to the highest irradiation environment are the entry and exit windows, the central tube surrounding the beam pipe and the mirror supports. However, the expected irradiation dose is not particularly high for the employed materials (epoxy, polymethacrylimide (PMI) foam, carbon fibre and polycarbonate (PC)) and the components are not under high mechanical stress. This lets to conclude that their functionalities will be still fulfilled, albeit with a slightly loss of mechanical performance due to radiation. The bonding of the mirrors with their supports is to be considered aside.

Although we do not expect surprises, it is planned to make an irradiation test using the same materials and process as the original assemblies. A safety factor of at least two in radiation levels with respect to the values shown in Table 5 will be used for testing [13].

Table 5: Material to be irradiated and the corresponding expected radiation levels.

Item	Radial position w.r.t beam	TID [kGy]	HEH [ $\times 10^{12}/\text{cm}^2$ ]	1 MeV $n_{eq}$ [ $\times 10^{12}/\text{cm}^2$ ]	Tests to be performed
Bonding of the mirror support to the mirror	>30 cm	$\sim 4$	$\sim 7$	$\sim 20$	Tensile test

Bonding tests have been performed to achieve reasonable stress on glass coupons. Fig. 15 shows such an assembly with a thin PTFE film to ensure a proper glue thickness on a delimited area.

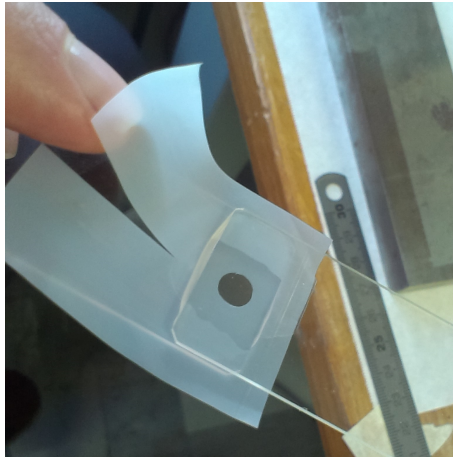


Figure 15: Coupon bonded for irradiation .

## References

- [1] The LHCb Collaboration, “Framework TDR for the LHCb Upgrade : Technical Design Report”, CERN-LHCC-2012-007 ; LHCb-TDR-12.
- [2] C. Frei, “RICH Infrastructure”, EDMS-1683369
- [3] The LHCb Collaboration, ”LHCb Upgraded RICH 1 Engineering Design Review Report”, LHCb-PUB-2016-XXX ; EDMS-1627005.
- [4] “Engineering Design Report for the Elementary Cell of the RICH photon detector”, EDMS-1627008
- [5] The LHCb Collaboration, “LHCb PID Upgrade Technical Design Report”, CERN-LHCC-2013-022 ; LHCb-TDR-014.
- [6] M. Adinolfi et al., “LHCb RICH2 Engineering Design Review Report”, LHCb-2002-009, March 2002.
- [7] M. Benettoni “RICH2 PDAs support mechanics and cooling” Presentation at the ”RICH Upgrade Meeting”, 9th September 2015, <https://indico.cern.ch/event/443766/>
- [8] C. Frei, “Cooling investigations for the RICH upgrade”, EDMS-1627009.
- [9] “Comparison of liquid coolants suitable for single-phase detector cooling.” <https://twiki.cern.ch/twiki/pub/LHCb/C6K/Coolants-review.pdf>
- [10] M. Karacson, “Radiation levels in the LHCb cavern”, Presentation at the “LHCb Upgrade Electronics” Meeting, February 2013, <https://indico.cern.ch/event/225746/>
- [11] M. Karacson, “Update on expected dose and fluence for the upgraded RICH”, Presentation at the “Meeting on Irradiations for RICH Upgrade”, February 2016, <https://indico.cern.ch/event/503375/>
- [12] M. Fiorini, “Plans for CLARO8v3 irradiation”, Presentation at the “Meeting on Irradiations for RICH Upgrade”, February 2016, <https://indico.cern.ch/event/503375/>
- [13] C. Frei, “RICH Upgrade Irradiation”, Presentation at the “Meeting on Irradiations for RICH Upgrade”, February 2016, <https://indico.cern.ch/event/503375/>